

## Accurate quantum mechanical treatment of phonon instability: body-centred cubic zirconium

This article has been downloaded from IOPscience. Please scroll down to see the full text article.

2002 J. Phys.: Condens. Matter 14 L695

(<http://iopscience.iop.org/0953-8984/14/43/101>)

View [the table of contents for this issue](#), or go to the [journal homepage](#) for more

Download details:

IP Address: 171.66.16.96

The article was downloaded on 18/05/2010 at 15:14

Please note that [terms and conditions apply](#).

## LETTER TO THE EDITOR

## Accurate quantum mechanical treatment of phonon instability: body-centred cubic zirconium

Y Wang<sup>1</sup>, R Ahuja<sup>1</sup>, M C Qian<sup>1</sup> and B Johansson<sup>1,2</sup><sup>1</sup> Condensed Matter Theory Group, Department of Physics, Uppsala University, Box 530, S-751 21, Uppsala, Sweden<sup>2</sup> Applied Materials Physics, Department of Materials Science and Engineering, Royal Institute of Technology, S-100 44, Stockholm, Sweden

Received 28 August 2002

Published 18 October 2002

Online at [stacks.iop.org/JPhysCM/14/L695](http://stacks.iop.org/JPhysCM/14/L695)**Abstract**

The  $T_1$  N point and  $\omega$  point phonon anomalies for body-centred cubic (bcc) Zr are studied using an approach which goes beyond the traditional quasi-harmonic approximation and perturbation theory. We are able to reproduce, for the first time, the anomalous phonon behaviour in bcc Zr.

The phonon anomaly in connection with martensitic transformations has been the topic of numerous experimental and theoretical studies [1–11] over the past few decades. However, a complete quantitative understanding of this subject based on lattice dynamics has still not been accomplished.

In the present theory of lattice dynamics, the central roles are played by the harmonic and the quasi-harmonic approximations [12, 13]. The lattice potential of the system is truncated at terms of second order in the atomic displacements; as a result, the normal-mode transformation allows the Hamiltonian of the system to be expressed as a sum of non-interacting one-dimensional harmonic Hamiltonians. The physical concept of ‘phonon’ is then introduced naturally, since the energy eigenvalue spectrum for a parabola-like potential consists of equally spaced energy levels which makes the energy excitation look like a simple increase in the number of particles. Many calculations [14–17] of the lattice dynamics have appeared, with very good agreement obtained with the observed phonon dispersion curves for the solid at low temperatures.

However, in the real physical world the systems do not always behave in the same manner. Exceptional cases include those of the transition metals of group 3 (Sc, Y, La) and group 4 (Ti, Zr, Hf) and their alloys, where the high-temperature body-centred cubic (bcc) phase exhibits intrinsic phonon anomalies tending towards the hexagonal close-packed and  $\omega$  structures. Inelastic neutron scattering measurements [1, 2, 5, 6] on bcc Zr and Zr alloys show that:

- (1) the transverse  $[1\bar{1}0]$  phonon at  $(1/2, 1/2, 0)$  (the  $T_1$  N point) as well as the longitudinal phonon at  $(2/3, 2/3, 2/3)$  (the so-called  $\omega$  point, equivalent to the  $TA_2$   $[\bar{1}11]$  phonon at  $(2/3, 1/3, 1/3)$ ) have very low frequencies, very broadly scattering line shapes, and strong quasielastic intensities;

- (2) the measured phonon spectrum and the quasielastic scattering indicate a strong asymmetry around the (2, 2, 2) bcc Bragg peak along the  $[11\bar{2}]$  direction which seems to violate the expected bcc symmetry and which was assumed to be associated with persistent  $\omega$  fluctuations [6, 7] in the bcc phase.

These results demonstrate a number of peculiarities of lattice vibrations, which do not agree with the conventional phonon picture.

Nowadays the rapid developments in both computer speed and computational methods have made it routine to perform accurate first-principles calculations of the lattice potential—total energy changes associated with atomic displacements at zero temperature [18–20]. For certain phonon modes, the harmonic approximation then yields an imaginary frequency [14, 21] which is somewhat difficult to understand in the proper sense of energetics. It is therefore natural to ask whether there is any interesting physics underlying these features. It seems to be necessary to go beyond the simple phonon picture and to give a precise solution for certain systems. This was first accomplished by Ho *et al* [22] for studying the vibrations of hydrogen isotopes in NbH and later applied by Elsässer *et al* [23] for weakly anharmonic vibrations of H in bcc NbH and for strongly anharmonic vibrations of H in fcc PdH.

In this letter our calculations are designed to study highly anharmonic phonons. We study the  $T_1$  N point and  $\omega$  point phonon anomalies for bcc Zr, by viewing the lattice mode as a one-dimensional periodic system of atoms. As will be seen, our results are most encouraging in that the measured phonon anomalies, which cannot be explained within the conventional harmonic approximation, are well reproduced in the framework of state-of-the-art, solid-state quantum mechanical calculations.

In the bcc metal [3], the  $T_1$  N point oscillation is formed by the shuffling of the two neighbouring  $\langle 110 \rangle$  planes along the  $[1\bar{1}0]$  direction. The  $\omega$  point oscillation is formed by the opposite movements of the two neighbouring  $\langle 111 \rangle$  planes and with every third plane staying at rest. Notice that the ‘moving atom’ has a periodic length of  $b = \sqrt{2}a$  ( $a$  is the bcc lattice constant) for the  $T_1$  N point oscillation and  $b = \sqrt{3}a$  for the  $\omega$  point oscillation. This forms a straightforward physical picture of an atom in a one-dimensional periodic lattice potential  $V(x)$  where  $x$  is the relative displacement between the moving adjacent planes. We can naturally solve this problem since it is analogous to a one-dimensional electronic energy band problem [24] in the form

$$\left[ \frac{\hbar^2 G^2}{2\mu} - \epsilon \right] C(G) + \sum_{G'} U(G - G') C(G') = 0, \quad (1)$$

where  $\hbar$  is the Dirac constant,  $\mu$  is the effective mass of a two-atom system,  $U(G)$  is the coefficient of the Fourier transform of  $V(x)$ , and  $C(G)$  is the coefficient of the linear combination of the ‘one-atom’ wavefunction with the plane-wave basis  $\exp(iGx)$ .

In order to obtain  $V(x)$ , the projector augmented-wave (PAW) method within the generalized gradient approximation (GGA) is employed. We use the Vienna *ab initio* simulation package (VASP) [20] with the high-precision choice and Monkhorst  $15 \times 15 \times 15$   $k$  points. With core radii of 2.5 au, the 4s4p5s4d shells have been treated as valence states.  $V(x)$  is calculated by a lattice displacement step of  $0.01b$  (meaning 51 points in the half-periodic length!) for the corresponding oscillation. Then more densely spaced points corresponding to lattice displacement steps of  $0.001b$  are derived by a cubic spline interpolation as the input to produce the coefficients of the fast Fourier transformation. The convergence was tested by varying the number of plane waves that are needed. We found that 500 ( $|b/2\pi G_{\max}| = 250$ ) plane waves were more than enough to give fully convergent results over the entire energy range examined in this letter.

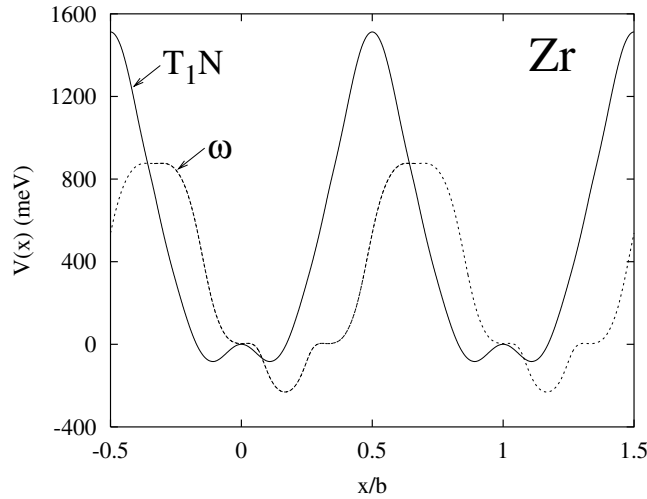


**Figure 1.** The calculated lattice potential  $V(x)$  for bcc Zr as a function of the displacements corresponding to the longitudinal phonon with  $q = (2\pi/a) (2/3, 2/3, 2/3)$  (solid curve) and the transverse  $T_1$  phonon with  $q = (2\pi/a) (1/2, 1/2, 0)$  (dashed curve).  $x$  is measured in units of the corresponding periodic lengths of displacements.

Figure 1 displays  $V(x)$ , calculated at the measured [1] 1423 K bcc lattice constant of 6.8445 au, for the  $T_1$  N point and  $\omega$  point oscillations as a function of the atomic displacements away from their static bcc crystal positions. Judging from the behaviours,  $V(x)$  is now too anomalous to be approximated by a parabola. Instead of being a local minimum, the atomic equilibrium position is located at the local peak top for the  $T_1$  N point oscillation and at a shoulder for the  $\omega$  point oscillation. It is widely accepted that the occurrence of these anomalies is closely connected to the detailed topology of the electronic bands near the Fermi energy—the electronic response to the ionic displacements.

Let us first focus on the energy eigenvalue spectra as the essential aspect for understanding the present approach relative to that of the quasi-harmonic approximation. In figures 2 and 3 we have plotted the energy eigenvalue spectra solved at the measured 1423 K bcc lattice constant of 6.8445 au, for the  $T_1$  N point and  $\omega$  point oscillations, respectively. The energy spacing (ES) between the adjacent energy levels is amazing. In the right columns of figures 2 and 3 the ESs are also plotted with the lowest one indicating the quantum zero-point energy. If the system were harmonic all the ESs would be exactly equal. This is roughly the case for the first few levels. However, with increasing energy the ESs begin to deviate from those of the harmonic treatment. In the case of the  $T_1$  N point, the ESs first decrease rapidly for only a few levels to a certain threshold and then increase. In the case of the  $\omega$  point, the ESs show a slight increase for a certain number of levels, then they decrease for a certain number of levels to a certain threshold, and then increase again.

In figure 4 we have illustrated the particle probability distributions for some selected energy levels. For the cases of the  $T_1$  N point oscillation, we found that the two big peaks from the level  $n = 0$  evolved and merged into one strong peak at level  $n = 16$  accompanied with some weak satellite peaks. In contrast, for the case of  $\omega$  point oscillation, we found that the single big peak from the level  $n = 0$  evolved and became split into two well-separated strong peaks at level  $n = 25$  accompanied by some weak satellite peaks. In fact, in the case of the  $T_1$  N point oscillation the eigen-energy of level  $n = 16$  is almost equal to the energy of

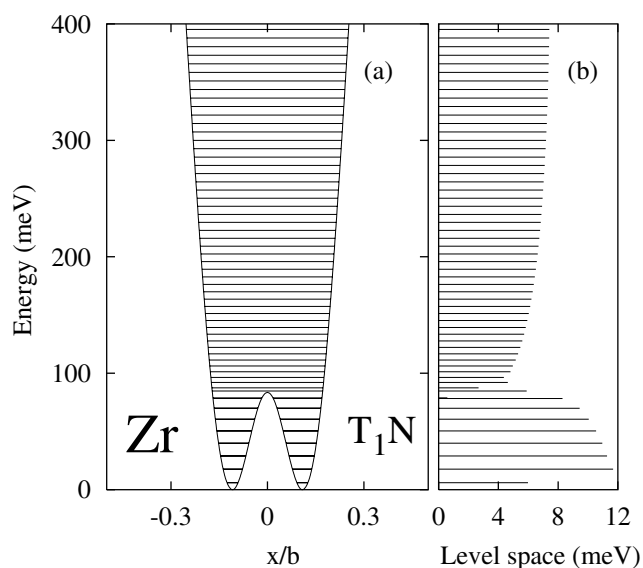


**Figure 2.** (a) The calculated energy eigenvalue spectra for the  $T_1 N$  point oscillation at the measured [1] 1423 K bcc lattice constant of 6.8445 au. (b) The corresponding energy space (shown by the widths of the horizontal lines) between the adjacent energy levels as a function of the energy eigenvalue, with the lowest one indicating the quantum zero-point energy.

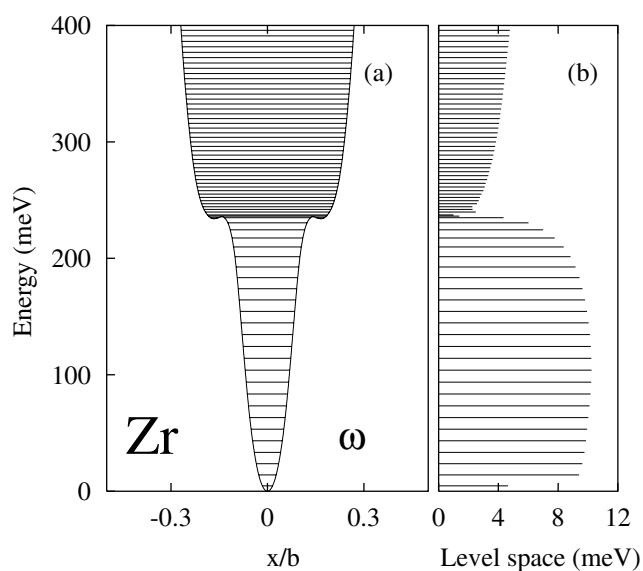


**Figure 3.** (a) The calculated energy eigenvalue spectra for the  $\omega$  point oscillation at the measured [1] 1423 K bcc lattice constant of 6.8445 au. (b) The corresponding energy space (shown by the widths of the horizontal lines) between the adjacent energy levels as a function of the energy eigenvalue. The lowest one corresponds to the quantum zero-point energy.

the central peak of  $V(x)$ , while in the case of the  $\omega$  point oscillation the eigen-energy of level  $n = 25$  is almost equal to the energy of the shoulders of  $V(x)$ .

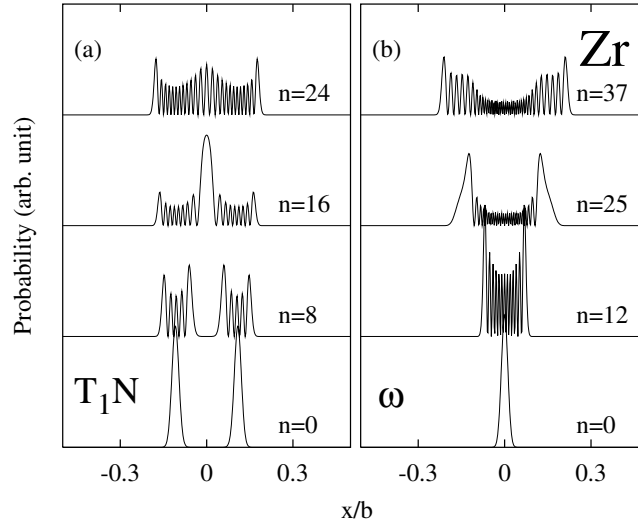


**Figure 4.** The calculated particle probability distributions for some selected energy levels: (a)  $T_1 N$  point oscillation; (b)  $\omega$  point oscillation.

Having discussed the mathematical properties, we turn to the interesting question regarding the energy absorption in the inelastic neutron scattering measurements [1, 2, 5, 6]. In doing this, we have assumed a very simplified perturbation of form  $\exp(i2\pi r/b)$  and used the following formula to calculate the energy absorption rate  $P(E)$  as a function of the energy  $E$ :

$$P(E) = \sum_{i < j} e^{-\beta \epsilon_i} \langle \varphi_i | e^{i2\pi r/b} | \varphi_j \rangle^2 e^{-(\epsilon_j - \epsilon_i - E)^2 / \sigma^2}, \quad (2)$$

where  $\beta = 1/k_B T$  with  $k_B$  being Boltzmann's constant and  $T$  being the temperature,  $\epsilon_i$  is the energy eigenvalue of the  $i$ th eigenstate  $\varphi_i$ , and  $\sigma$  (we use a value of 0.2 meV in this letter) is the Gaussian widening representing the precision of the experimental instruments. We have calculated  $P(E)$  at  $T = 1168, 1423,$  and  $1883$  K at the corresponding experimental lattice constant [1]. The results are plotted in the left and the right columns of figure 5, respectively, for the  $T_1 N$  point and the  $\omega$  point oscillations of Zr.

From figure 5, we find that, in good agreement with experiment, the calculated energy absorption has very low frequencies and the major absorption peak is very broad for both the  $T_1 N$  point and the  $\omega$  point oscillations. The numerical agreement between the calculation and the experiment is also good. For example, the major energy absorption is calculated to be in the range of 4–8 meV compared with the experimental peak positions of 4.48–6.91 meV (note the large errors in the fitting of the experimental work [1] by means of the so-called damped oscillator) for the  $T_1 N$  point oscillation. In the case of the  $T_1 N$  point oscillation, figure 5 also shows an absorption at zero energy. This is attributed to the pseudo-degeneracy of the lowest few levels in the double wells of  $V(x)$  (see figure 2). The experimental work by Heiming *et al* [1] indeed mentioned that inelastic intensity can be found down to zero energy transfer.

The more striking result obtained by our calculation is that, for the  $\omega$  point oscillation, an additional peak appears at 10 meV. The intensity of this peak decreases with increasing temperature but is still strong at  $T = 1883$  K, the highest temperature that we have considered. Strong support for this result is provided by the experimental results [5, 6] for the  $Zr_{1-x}Nb_x$  ( $x = 0.08$ – $0.2$ ) alloys in the bcc phase which indicate that the  $TA_2$  branch is split into two sub-branches. A better understanding of this can also be derived from figure 3 where the ESs

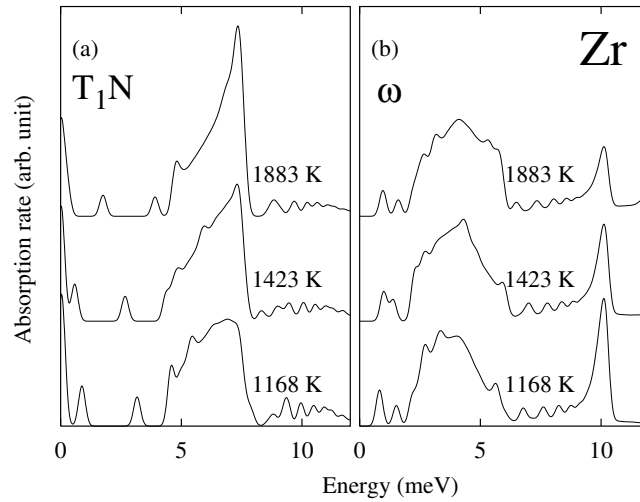


**Figure 5.** The calculated energy absorption rate as a function of the neutron energy: (a)  $T_1 N$  point oscillation; (b)  $\omega$  point oscillation.

are roughly partitioned into two groups positioned at around 4 and 10 meV. Zhang *et al* [7] argued that the  $T_1 N$  point oscillation for Zr should show a similar behaviour. However, our calculation (see the left columns of figures 5 and 2) shows that for the  $T_1 N$  point oscillation the peak at 10 meV is too weak to be observed since there are too few levels around 10 meV as compared with the case for the  $\omega$  point oscillation.

In summary, on the basis of first-principles calculations, we have answered the long-standing question about the phonon instabilities for the  $T_1 N$  point and the  $\omega$  point oscillations of Zr which are the well-known representative cases of high-temperature martensitic transformations. In our approach the lattice potential (the electronic total energy) for the atomic displacement pattern corresponding to a given phonon is first calculated. Unlike in the harmonic approximation, where the atomic displacements are kept small and only the quadratic term is extracted, in the new approach the displacements cover the whole range of periodicity determined by a given phonon, and no higher-order truncation is needed. In the next step a one-dimensional Schrödinger equation for the quantum motion of atoms (in a given phonon mode) is solved, drawing analogies to one-dimensional electronic band theory.

This work was supported by the Swedish Foundation for Strategic Research (SSF), Swedish Natural Science Research Council (NFR), and Göran Gustafsson Foundation.

## References

- [1] Heiming A, Petry W, Trampenau J, Alba M, Herzig C, Schober H R and Vogl G 1991 *Phys. Rev. B* **43** 10948
- [2] Dubos O, Petry W, Neuhaus J and Hennion B 1998 *Eur. Phys. J. B* **3** 447
- [3] Petry W, Heiming A, Trampenau J, Alba M, Herzig C, Schober H R and Vogl G 1991 *Phys. Rev. B* **43** 10933
- [4] Petry W, Heiming A, Trampenau J, Alba M and Vogl G 1989 *Physica B* **156/157** 56  
Güthoff F, Petry W, Stassis C, Heiming A, Hennion B, Herzig C and Trampenau J 1993 *Phys. Rev. B* **47** 2563  
Petry W, Trampenau J and Herzig C 1993 *Phys. Rev. B* **48** 881
- [5] Axe J D, Keating D T and Moss S C 1975 *Phys. Rev. Lett.* **35** 530
- [6] Noda Y, Yamada Y and Shapiro S M 1989 *Phys. Rev. B* **40** 5995
- [7] Zhang B L, Wang C Z, Ho K M, Turner D and Ye Y Y 1995 *Phys. Rev. Lett.* **74** 1375
- [8] Sanati M, Saxena A and Lookman T 2002 *Phys. Rev. B* **64** 092101

- 
- [9] Morris J R and Ho K M 2001 *Phys. Rev. B* **63** 224116
  - [10] Porta M and Castán T 2001 *Phys. Rev. B* **63** 134104
  - [11] Pinsook U and Ackland G J 1999 *Phys. Rev. B* **59** 13642
  - [12] Born M and Huang K 1956 *Dynamical Theory of Crystal Lattice* (London: Oxford University Press)
  - [13] Foreman A J E and Lomer W M 1957 *Proc. Phys. Soc. B* **70** 1143
  - [14] Dewhurst J K, Ahuja R, Li S and Johansson B 2002 *Phys. Rev. Lett.* **88** 075504
  - [15] Li Z and Tse J S 2000 *Phys. Rev. Lett.* **85** 5130
  - [16] Debernardi A, Alouani M and Dreyssé H 2001 *Phys. Rev. B* **63** 064305
  - [17] Frank W, Elsässer C and Fähnle M 1995 *Phys. Rev. Lett.* **74** 1791
  - [18] Ho K M, Fu C L and Harmon N 1984 *Phys. Rev. B* **29** 1575
  - [19] Grad G B, Blaha P, Luitz J, Schwarz K, Guillermet A F and Sferco S J 2000 *Phys. Rev. B* **62** 12743
  - [20] Kresse G and Joubert J 1999 *Phys. Rev. B* **59** 1758
  - [21] Persson K, Ekman M and Ozoliņš V 2000 *Phys. Rev. B* **61** 11221
  - [22] Ho K M, Tao H J and Zhu X Y 1984 *Phys. Rev. Lett.* **53** 1586  
Tao H J, Ho K M and Zhu X Y 1986 *Phys. Rev. B* **34** 8394
  - [23] Elsässer C, Ho K M, Chan C T and Fähnle M 1991 *Phys. Rev. B* **44** 10377  
Elsässer C, Ho K M, Chan C T and Fähnle M 1992 *J. Phys.: Condens. Matter* **4** 5207
  - [24] Kittel C 1996 *Solid State Physics* (New York: Wiley)